

# Statistical implications of relaxing the homogeneous mixing assumption in time series Susceptible-Infectious-Removed models

Luis D. J. Martinez Lomeli<sup>1</sup>, Michelle N. Ngo<sup>1</sup>, Jon Wakefield<sup>2</sup>, Babak Shahbaba<sup>1,3,\*</sup>, Vladimir N. Minin<sup>1,3,\*</sup>

<sup>1</sup>Center for Complex Biological Systems, University of California, Irvine.

<sup>2</sup>Departments of Biostatistics and Statistics, University of Washington, Seattle, Washington

<sup>3</sup>Department of Statistics, University of California, Irvine

\*corresponding authors: babaks@uci.edu, vminin@uci.edu

## Abstract

Infectious disease epidemiologists routinely fit stochastic epidemic models to time series data to elucidate infectious disease dynamics, evaluate interventions, and forecast epidemic trajectories. To improve computational tractability, many approximate stochastic models have been proposed. In this paper, we focus on one class of such approximations — time series Susceptible-Infectious-Removed (TSIR) models. Infectious disease modeling often starts with a homogeneous mixing assumption, postulating that the rate of disease transmission is proportional to a product of the numbers of susceptible and infectious individuals. One popular way to relax this assumption proceeds by raising the number of susceptible and/or infectious individuals to some positive powers. We show that when this technique is used within the TSIR models they cannot be interpreted as approximate SIR models, which has important implications for TSIR-based statistical inference. Our simulation study shows that TSIR-based estimates of infection and mixing rates are systematically biased in the presence of non-homogeneous mixing, suggesting that caution is needed when interpreting TSIR model parameter estimates when this class of models relaxes the homogeneous mixing assumption.

## 1 Introduction

Susceptible-Infectious-Recovered (SIR) models, first presented by Kermack and McKendrick (1927), are commonly used to capture the dynamics of an infectious disease outbreak in a population. Stochastic versions of SIR-like models tend to be difficult to fit due to computational intractability of the likelihood function. One solution to circumvent this issue is to use time series SIR models (TSIR) (Finkenstädt and Grenfell, 2000; Becker and Grenfell, 2017; Baker et al., 2019; Giles et al., 2020, 2021), which are based on a branching process approximation of the epidemic progression. Although the branching process approximation of the TSIR model has a rigorous mathematical justification, its validity breaks down when the assumption of homogeneous mixing (also known as the law of mass action) is relaxed. This could lead to an unjustifiable model misspecification. In this paper, we investigate the statistical implications of such model misspecification and find that the TSIR model with non-homogeneous mixing can produce biased estimates of the infection rates.

Fitting stochastic epidemic models to empirical data within a likelihood-based framework is a challenging task because it requires integrating over a large number of missing data, which is computationally burdensome. Methods that approximate the likelihood function improve the computational tractability have a long history in infectious disease modeling. Discrete time models that move individuals across multiple compartments provide one class of such approximate methods (Longini Jr and Koopman, 1982; Lekone and Finkenstädt, 2006; Held and Paul, 2012). While these approximate models are tractable, they rely on several simplifying assumptions that make them harder to apply to more general settings, for example, when data are collected at uneven observation times. Particle filter optimization and Markov chain Monte Carlo (MCMC) approaches offer another solution to the intractable likelihood problem in maximum likelihood and Bayesian framework (Andrieu et al., 2010; Ionides et al., 2011, 2015; Dukic et al., 2012; Koepke et al., 2016). However, particle filter methods are computationally expensive and can suffer from particle impoverishment problems. Although more general data augmentation MCMC approaches have been successfully applied to epidemic models, in some cases, it is necessary to impute more unknown variables than is feasible in practice (Cauchemez et al., 2004; Jewell et al., 2009; O’Neill,

2010; Fintzi et al., 2017). Finally, problems with intractable likelihoods can be tackled by Approximate Bayesian Computation methods, these approaches are computationally intensive, with performance being sensitive to the type of summary statistics used (McKinley et al., 2009; Toni et al., 2009; Owen et al., 2015).

We are interested in the TSIR family of models that provide a simple approximation to the SIR process, allowing for analysis of incidence data (the most common type of surveillance data reported), and remain tractable when extended to simultaneous modeling of multiple geographic locations (Xia et al., 2004; Jandarov et al., 2014; Wakefield et al., 2019). In particular, the likelihood function takes the form of a product of negative binomial probabilities when the number of infections in a population is approximated by a linear birth process under the assumption of homogeneous mixing (Feller, 1968; Allen, 2010). This negative binomial-based approximation is commonly generalized to non-homogeneous mixing, but this generalization has not been rigorously justified and its statistical implications are yet to be explored.

In this work, we study statistical implications of TSIR under non-homogeneous mixing using recent computational advances of fitting Bayesian SIR models to data, to which we refer to as *BayesSIR* (Ho et al., 2018a). The main contributions of the paper are as follows: (1) We show where the TSIR branching process approximation fails when applied to dynamics with non-homogeneous mixing and provide numerical evidence for the persisting discrepancy between the transition probabilities of TSIR and SIR models; (2) we provide a detailed analysis of the model misspecification effect by comparing the performance of BayesSIR to our Bayesian implementation of the TSIR model with the negative binomial-based likelihood, to which we refer as *BayesTSIR*. Using synthetic data, we show that disagreement between BayesTSIR-based and BayesSIR-based inference can be substantial; (3) we extend the *BayesSIR* model to allow for time-varying infection rates in order to provide a rigorous framework for modeling incidence time series data routinely collected during infectious disease surveillance. We show that the discrepancies between *BayesSIR* and *BayesTSIR* still persist in this setting.

In the last contribution, we apply our generalization of *BayesSIR* with time-varying infection rates to the analysis of the historical London measles dataset that contains biweekly incidence records collected before the implementation of vaccination campaigns. In this dataset, the measles time series shows a seasonal pattern, where higher case numbers were reported during school-term months compared to school breaks. To account for this pattern, we consider two ways in which the infection rate can vary throughout the year: (1) with two infection rates, shared across years, corresponding to school-term and school-break, and (2) with rates that vary biweekly throughout each year, but the same biweekly period has the same infection rate across years. Our results show that infection rate estimates produced by the BayesSIR with non-homogeneous mixing fluctuate less throughout a year than the analogous estimates produced by the BayesTSIR model, suggesting presence of substantial biases in BayesTSIR-based estimates caused by the TSIR approximation.

## 2 Methods

### 2.1 Incidence Epidemic Data

Suppose we observe a time series of an infectious disease incidence  $\mathbf{Z} = \{Z_1, \dots, Z_n\}$ , where  $Z_i$  represents the number of new cases reported in a period  $i$  (e.g., period length could be a week). We would like to infer the dynamics of the infectious disease spread. For this purpose, we follow the TSIR model assumptions and postulate that all individuals infected in the period  $i$  will recover at the end of this period. This means that  $\mathbf{Z}$  can be thought of as underreported disease prevalence, defined as the number of infectious/infected individuals in each period. Therefore, to proceed with statistical inference we need a model for changes in the actual prevalence.

## 2.2 Stochastic SIR Model

We use a Susceptible-Infectious-Removed (SIR) process to model the prevalence dynamics, including a modification that allows for non-homogeneous mixing. More specifically, we define a continuous-time stochastic process  $\mathbf{X}(t) = \{S(t), I(t)\}_{t \geq 0}$ , where  $S(t)$  and  $I(t)$  denote the numbers of susceptible and infectious individuals at time  $t$  respectively. Given a population of size  $N$  with no demographic changes (births, deaths, migration, etc.), and for a small time interval  $(t, t + \Delta t)$ , the possible events that can occur are (1) a new infection of a susceptible person, (2) a new recovery of an infectious individual, or (3) no change in the population. These events have the following associated probabilities:

$$\mathbb{P}[\mathbf{X}(t + \Delta t) = (k, l) \mid \mathbf{X}(t) = (s, i)] = \begin{cases} \frac{\beta}{N} s i^\alpha \Delta t + o(\Delta t) & (k, l) = (s - 1, i + 1), \\ \gamma i \Delta t + o(\Delta t) & (k, l) = (s, i - 1), \\ 1 - (\frac{\beta}{N} s i^\alpha + \gamma i) \Delta t + o(\Delta t) & (k, l) = (s, i), \\ o(\Delta t) & \text{otherwise,} \end{cases} \quad (1)$$

where  $\beta$  and  $\gamma$  are the infection and recovery rates respectively, and  $\alpha$  represents the mixing parameter for non-homogeneous dynamics. In the classical SIR model, the mixing rate is assumed to be  $\alpha = 1$ , corresponding to the assumption of homogeneous mixing. By setting  $\alpha < 1$  we make the infection rate slower than it would be in the classical SIR, which is reasonable if we expect that susceptible and infectious individuals are not coming into contact with each other as freely as they would be under the homogeneous mixing assumption. Note that the model only keeps track of the number of susceptible and infectious individuals but it is possible to obtain the number of individuals in the recovered compartment, since at all times it is assumed that the three compartment sizes add up to the population size  $N$ .

We extend the SIR process to model the infection process across multiple periods of time where the infection rate can vary per period. For example, we can consider a single infection rate per month, season, or year. This implies that the vector of SIR parameters across all the observation periods of interest can be written as

$$\boldsymbol{\theta} = (\alpha, \beta_1, \dots, \beta_k, \gamma)^t, \quad (2)$$

where  $\beta_j$  represents the infection rate at the  $j$ -th set of time intervals, with  $j = 1, \dots, k$ , and  $k$  represents the total number of different infection rates allowed in the model. This means that for the  $i$ -th observation period, the corresponding SIR process is parameterized by  $(\alpha, \beta_i, \gamma)^t$ , where some  $\beta$ s may be constrained to be equal across observation periods.

## 2.3 Parameters Inference

If we want to proceed in a Bayesian framework, then ideally we would like to approximate the posterior distribution of the SIR parameters  $\boldsymbol{\theta}$ , the true susceptibles  $\mathbf{S}$ , and true infectious  $\mathbf{I}$  subpopulations, given by:

$$p(\boldsymbol{\theta}, \mathbf{S}, \mathbf{I} \mid \mathbf{Z}) \propto p(\mathbf{Z} \mid \mathbf{S}, \mathbf{I}) \cdot p(\mathbf{S}, \mathbf{I} \mid \boldsymbol{\theta}) \cdot p(\boldsymbol{\theta}), \quad (3)$$

where  $\mathbf{S} = (S_1, \dots, S_n)^t$ ,  $\mathbf{I} = (I_1, \dots, I_n)^t$  and  $\mathbf{Z}$  represents the vector of incidence records. However, approximating the posterior distribution (3) is a difficult computational problem since the values for  $\mathbf{S}$  and  $\mathbf{I}$  are discrete and high dimensional.

In general, the imputation of  $\mathbf{S}$  and  $\mathbf{I}$  can not be done but techniques exist for endemic infectious diseases under certain assumptions. In particular, TSIR provides an ingenious method to estimate  $\tilde{\mathbf{S}} = (\tilde{S}_1, \dots, \tilde{S}_n)^t$  and  $\tilde{\mathbf{I}} = (\tilde{I}_1, \dots, \tilde{I}_n)^t$  from  $\mathbf{Z}$ . This method relies on the assumption that incidence and prevalence are close enough to be considered almost identical at any observation time, since the observation times are approximately equal to the infectious period. Also, it is assumed that information about new births in the population is available along with the incidence records. Following these assumptions, TSIR provides a reconstruction of the susceptible dynamics based on a recursive model that accounts for births, new infections and a reporting probability. Then, a regression model is derived

between the cumulative sum of births and the cumulative sum of cases. The slope of this model is interpreted as the reporting rate,  $\rho$ , from which the true cases are estimated. The full description of the TSIR model can be found in (Finkenstädt and Grenfell, 2000).

After  $\tilde{\mathbf{S}}$  and  $\tilde{\mathbf{I}}$  are estimated, we approximate the posterior distribution of the SIR model parameters using

$$p(\boldsymbol{\theta}|\mathbf{Y}) \propto p(\mathbf{Y}|\boldsymbol{\theta}) \cdot p(\boldsymbol{\theta}), \quad (4)$$

where  $\mathbf{Y} = (\tilde{\mathbf{S}}, \tilde{\mathbf{I}})$ , and  $p(\boldsymbol{\theta})$  represents the prior distribution over the SIR model parameters.

## 2.4 SIR likelihood function

The likelihood function from equation (4) can be written as the product of the Markov process transition probabilities

$$p(\mathbf{Y}|\boldsymbol{\theta}) = \prod_{t=1}^{n-1} P_{\mathbf{X}_t, \mathbf{X}_{t+1}}(\Delta t), \quad (5)$$

where the transition probabilities are

$$P_{\mathbf{X}_t, \mathbf{X}_{t+1}}(\Delta t) = \mathbb{P}[\mathbf{X}(t + \Delta t) = \{\tilde{S}_{t+1}, \tilde{I}_{t+1}\} | \mathbf{X}(t) = \{\tilde{S}_t, \tilde{I}_t\}]. \quad (6)$$

With the exception of the most simple cases (Feller, 1968; Allen, 2010), statistical inference involving these transition probabilities can be quite difficult. A common approach is to solve the forward Kolmogorov equations by matrix exponentiation techniques. However, these techniques can be computationally prohibitive for stochastic systems with a large number of states such as SIR models (Keeling and Ross, 2008). Instead, we consider two alternative approaches where the exact transition probabilities are calculated: using a negative binomial approximation for the infection process which is part of the TSIR formulation, and using a highly accurate numerical approximation technique that explores the fact that the the SIR model can be represented by a death/birth-death process (Ho et al., 2018b,a).

### 2.4.1 Negative binomial approximation to the transition probabilities.

A negative binomial distribution model has been previously adopted by the TSIR framework to approximate SIR transition probabilities (Grenfell et al., 2002; Bjørnstad and Grenfell, 2008). This model is derived via a linear pure birth approximation of the SIR model, as summarized in (Wakefield et al., 2019), and provides a simple expression to calculate the transition probabilities (6). In this derivation, the law of mass action assumption of homogeneous mixing among susceptible and infectious individuals is required. More specifically, one assumes the number of susceptible individuals is approximately constant ( $S(t) = s$ ) during the time period of interest and the number of infectious individuals follows a pure birth process:

$$\mathbb{P}(I(t + \Delta t) = j | I(t) = i) = \begin{cases} \frac{\beta}{N} s i^\alpha + o(\Delta t) & \text{if } j = i + 1, \\ o(\Delta t) & \text{otherwise.} \end{cases} \quad (7)$$

When  $\alpha = 1$ , properties of the *linear* pure-birth process imply that the number of infectious individuals at time  $t$ , given the number of susceptible and infectious individuals at  $t - 1$ , can be written as

$$I_t | (S_{t-1}, I_{t-1}) \sim \text{NegBin}(m_t, I_{t-1}), \quad (8)$$

where the mean of the distribution is

$$m_t = I_{t-1} \left( e^{\beta S_{t-1}/N} - 1 \right). \quad (9)$$

TSIR models use the first order Taylor expansion of equation (9) and write the mean of the negative binomial model (8) as

$$m_t = \beta S_{t-1} I_{t-1} / N. \quad (10)$$

Previous literature assumes this model can be generalized to allow for non-homogeneous mixing simply by raising the infectious population to a mixing power,  $\alpha$ , in the mean of the distribution,  $m_t = \beta S_{t-1} I_{t-1}^\alpha / N$  (Finkenstädt and Grenfell, 2000; Grenfell et al., 2002). This modification can also be applied to equation (9) to obtain  $m_t = I_{t-1}^\alpha (e^{\beta S_{t-1} / N} - 1)$ . However, neither of these approximations are mathematically justified, because the negative binomial approximation of SIR transition probabilities arises from the linear birth approximation and is valid only when  $\alpha = 1$ . This incorrect generalization can lead to model misspecification as we show in Section 3. Also, note that since the negative binomial model was derived using a linear birth approximation, this model should be valid under pure birth conditions, which corresponds to the case when the size of the susceptible population is significantly larger than the number of infectious individuals. One example of this setting is the beginning of an epidemic outbreak where the infectious population grows exponentially. Finally, within the context of TSIR, since the time between observations is assumed to match the infectious period of a disease, the negative binomial model does not consider recovery events; thus, the recovery rate should be approximately one and is not estimated.

#### 2.4.2 Numerical approximation of the transition probabilities

Recently, numerical algorithms for birth/birth-death processes has been introduced to efficiently evaluate finite time transition probabilities of these bivariate stochastic processes (Ho et al., 2018b,a). This class of processes contains the SIR model (1) when it is expressed as a death/birth-death process (Figure S-1). The idea is to reparameterize the SIR process in terms of the cumulative number of infections,  $nSI(t)$ , and the cumulative number of removals,  $nIR(t)$ . The original random variables  $S(t)$  and  $I(t)$  can be recovered deterministically from  $nSI(t)$ ,  $nIR(t)$ ,  $S(0)$ , and  $I(0)$ . For the case of a SIR process with this alternative parametrization, the `MultiBD` package in R provides an efficient and numerically stable implementation for the calculation of the transition probabilities required for direct likelihood based inference. This means that if we are able to reconstruct the susceptible and infectious populations from incidence records, we can estimate the posterior distribution of the model parameters  $\theta$  (4) using standard MCMC methods. The `MultiBD` package is able to calculate the required transition probabilities needed to execute an MCMC algorithm.

We also use the `MultiBD` exact method to compute transition probabilities of the non-linear pure birth process (7). In this pure birth regime, the `MultiBD` exact method matches the Negative Binomial probabilities from Equation (8) when  $\alpha = 1$  in (7). However, the negative binomial model returns incorrect transition probabilities when the mixing rate differs from unity as we show in Section 3.

### 2.5 Methods Summary

Starting from incidence data, we follow the TSIR approach to reconstruct the time series of susceptible and true cases. Then, to evaluate the likelihood function (equation (5)), we compute the required transition probabilities (equation (6)). In particular, for `BayesTSIR`, we obtain transition probabilities using the negative binomial distribution defined by equations (8) and (10). We also compute transition probabilities of the non-linear pure birth process (7). When we use these transition probabilities in Bayesian inference, we call the corresponding statistical method *BayesPureBirth*. For *BayesSIR*, we compute the transition probabilities using the exact method by Ho et al. (2018b,a). Finally, using the three Bayesian inference approaches, we approximate the posterior distribution of the model parameters (4) using MCMC methods. We summarize all transition probability approximations and the corresponding names of inferential procedures in Table 1. The source code for the computational implementations in this paper can be found at <https://github.com/luisdm1/BayesSIR>. Also, a slight

Table 1: Summary of statistical methods. We show the method names, the transition probabilities method, computational implementation and reference to the section in the main text where they are introduced.

Method	Transition Probabilities	Description	Section
<i>BayesSIR</i>	MultiBD-SIR	Exact method	2.4.2
<i>BayesPureBirth</i>	MultiBD-PureBirth	Exact method	2.4.2
<i>BayesTSIR</i>	NegBin	Negative binomial	2.4.1
NA	NegBinExp	Exponential negative binomial	2.4.1

extension of the `MultiBD` package to compute pure birth process transition probabilities can be found at <https://github.com/vnminin/MultiBDPureBirth2>.

### 3 Results

In this section, we first show conditions under which transition probabilities under different approximations take on similar values. We then provide insights about when these approximations diverge from each other and from exact calculations. Next, we compare the performance of our Bayesian implementation of the TSIR negative binomial model (*BayesTSIR*) and the SIR model with constant and time-varying infection rates (*BayesSIR*) for estimating mixing, infection, and removal rates. We apply our method to simulated prevalence data, and to a benchmark dataset from historic incidence measles records. When analyzing simulated data, we also include results of the *BayesPureBirth* method to unambiguously demonstrate that differences between *BayesTSIR* and *BayesSIR* methods cannot be explained by the pure birth approximation alone. Our results show that using *BayesTSIR* model results in potential bias in the parameter estimates and suggests exaggerated fluctuations of the infection rate estimates across time.

#### 3.1 Transition probabilities comparison

Our approach to the likelihood-based inference for prevalence and incidence data relies on the calculation of the transition probabilities shown in equation (6). However, model misspecification can lead to incorrect calculation of the these transition probabilities and severely impact the estimation of infection, removal and mixing rates. This can occur under the negative binomial model because it only considers new infections (births) but no removals. Therefore, the negative binomial model should be valid under a pure birth regime when the number of susceptible individuals does not change substantially and when the number of removals is negligible. For instance, these conditions occur at the beginning of an epidemic outbreak where there is an exponential growth phase of the number of new infections and the time period of interest is short. In this regime, the NegBin (*BayesTSIR*), PureBirth (*BayesPureBirth*), and SIR (*BayesSIR*) methods produce similar transition probabilities as observed in the right plot of Figure 1. This is due to the fact that new infections are more likely to occur than removals when the population of susceptible individuals is larger than the number of infectious cases, which induces a small effective removal rate  $\gamma I$ . Note that this can also occur when the removal rate  $\gamma$  is small. In contrast, when the recovery rate is large, there is a mismatch between the transition probabilities obtained using the exact `MultiBD` method and pure birth approximations since new removals are now more likely to occur. Since in these numerical experiments we assume that  $\alpha = 1$ , PureBirth and NegBinExp transition probabilities coincide exactly, as predicted by theory. Moreover, these distributions do not change when varying the removal rate since, by definition, these methods do not model this type of events as explained in Section 2.

Next, we compare transition probability calculation methods when varying both removal rate  $\gamma$  and mixing rate  $\alpha$ . When we consider non-homogeneous mixing ( $\alpha \neq 1$ ) under a pure birth regime, the NegBin and SIR transition probabilities are relatively close to each other when the recovery rate is small

## Transition probabilities under pure birth conditions

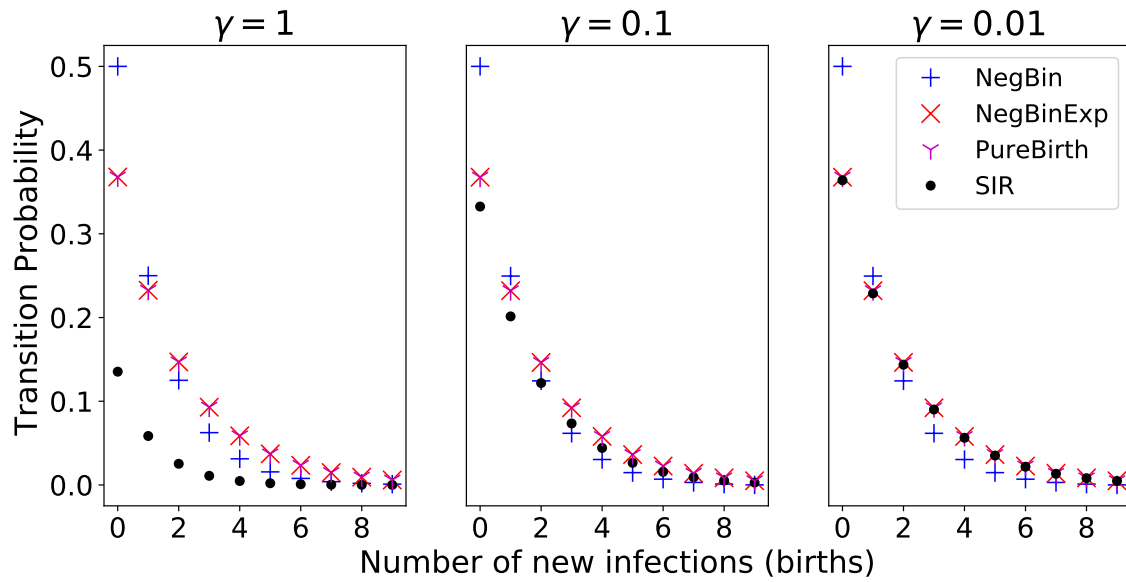


Figure 1: Comparison of the transition probabilities (equation (6)) using the two formulations of the negative binomial model (equations (9), (10)), a pure birth process and a SIR process when the recovery rate,  $\gamma$ , is decreased. Starting from an initial condition with  $(S_0 = 999999, I_0 = 1, R_0 = 0)$ , the plots show the probability of obtaining  $i \in \{0, 1, \dots, 9\}$  new infections (interpreted as new births in the linear birth approximation from TSIR). We assume a time step  $\Delta t = 1$ , homogeneous mixing,  $\alpha = 1$ , constant infection rate,  $\beta = 1$ . Also, we assume no recoveries,  $nIR = 0$ , in the MultiBD parametrization of the SIR process and in the pure birth approximation.

## Non-homogeneous mixing effect on the transition probabilities

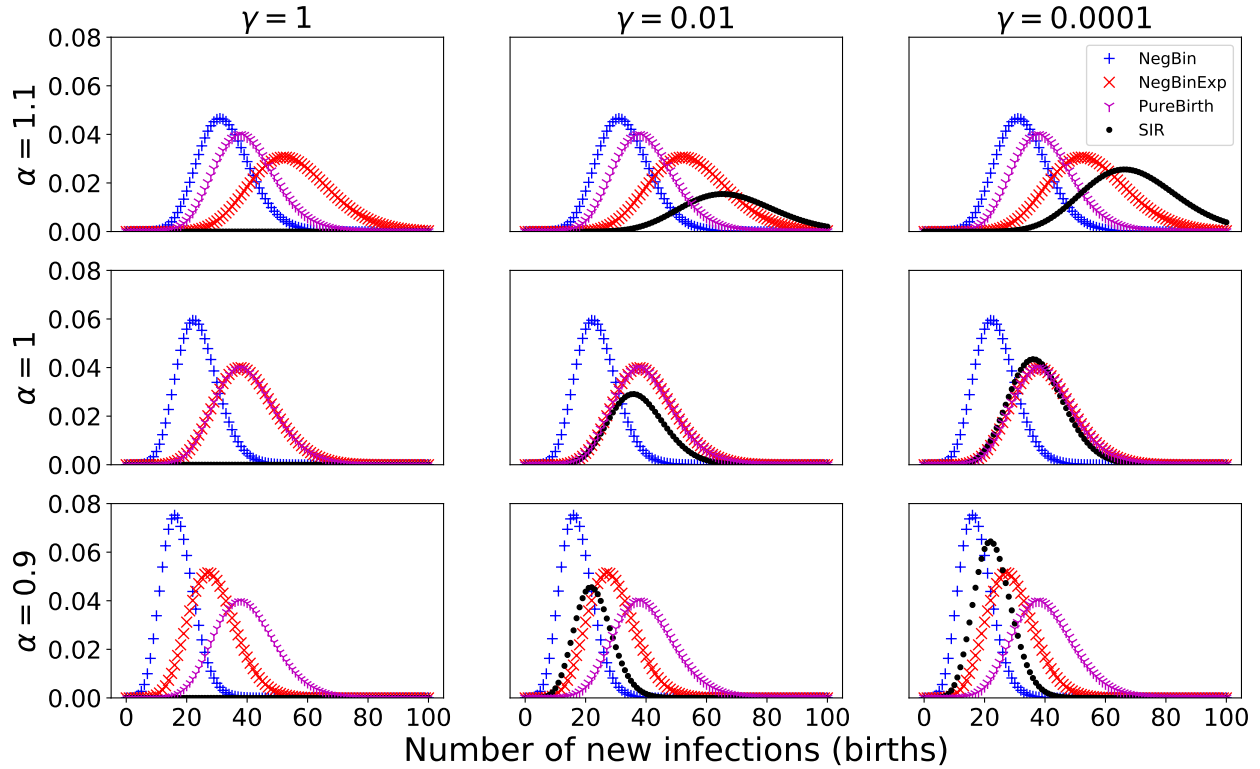


Figure 2: Comparison of the transition probabilities (equation (6)) using the two formulations of the negative binomial model (equations (9), (10)), a pure birth process and a SIR process. Here, we show the effect of non-homogeneous mixing on the transition probabilities by decreasing the mixing rate  $\alpha \in \{1.1, 1, 0.9\}$  and the recovery rate,  $\gamma \in \{1, 0.01, 0.0001\}$ . The time step is  $\Delta t = 1$ , the number of recoveries is  $nIR = 0$ , the infectious rate is set to  $\beta = 1$ , and the initial conditions for the SIR compartments are  $(S_0 = 500, I_0 = 25, R_0 = 0)$ .



as shown in Figure 2. However, as  $\gamma$  increases, there is a significant mismatch between the NegBin and SIR transition probabilities. For the pure birth models, we see that NegBinExp and PureBirth show equivalent transition probabilities during homogeneous mixing only. This shows that negative binomial models do not adequately approximate non-homogeneous mixing even under the pure birth regime. Finally, we observe in Figure 2 the mechanistic effect of the mixing rate on the transition probabilities distribution, i.e. this parameter can accelerate or delay the infection dynamics due to its non-linear effect on the rate of accumulation of new infections given by  $\beta S I^\alpha/N$ . As a result, the distribution of the transition probabilities can be shifted lower or higher when  $\alpha < 1$  or  $\alpha > 1$  respectively.

### 3.2 Inference using prevalence data

When prevalence data is available and sizes of the susceptible and removal compartments are known, it is possible to estimate the parameters of a SIR model using the direct likelihood calculations afforded by the analytical Negative Binomial formula under the BayesTSIR model and exact transition probability calculations under BayesPureBirth and BayesSIR models (Section 2). To illustrate this approach, we simulate stochastic SIR trajectories using the Gillespie algorithm and fixing the initial conditions to  $(S_0 = 999, I_0 = 1, R_0 = 0)$  and the SIR model parameters  $\beta = 0.0045$  and  $\gamma = 1$ . The effect of non-homogeneous mixing is implemented by setting  $\alpha = 0.8$ .

We show in Figure 3 the joint posterior distributions of the extended SIR mixing parameter ( $\alpha$ ) and infection rate ( $\beta$ ) obtained by analyzing one simulated data set shown in the same figure. As expected, the BayesSIR method successfully recovers the true parameters values. Interestingly, the BayesPureBirth method produces a posterior distribution that is similar in shape to the BayesSIR distribution, but shifted away from the true values. Nonetheless, the marginal posterior distributions of  $\alpha$ ) and  $\beta$  look reasonable even in this example. BayesTSIR posterior is centered far from the true parameters, but its large spread along the  $\beta$  axis allows it capture the true parameter values in the tail of the distribution.

To investigate frequentist properties of the above Bayesian methods, we performed a simulation study by generating an ensemble of 629 SIR simulations with fixed parameters under inhomogeneous mixing. At each iteration, a synthetic SIR trajectory was generated using the Gillespie algorithm until the depletion of the infectious compartment and values of the resulting SIR trajectories were recorded at a regular grid of time points. For each simulated trajectory, we performed a MCMC simulation to approximate the posterior distribution of the model parameters for each of the three methods: BayesSIR, BayesPureBirth and BayesTSIR. We report root mean squared errors (RMSEs), mean widths of 95% Bayesian credible intervals (BCIc), and coverage of 80%, 90%, and 95% BCIs in Table 2. BayesPureBirth and BayesSIR have similar RMSEs and BCI widths for  $\alpha$  and  $\beta$ . However, only BayesSIR BCI coverages are close to their nominal values. BayesPureBirth BCI coverages are significantly lower. BayesTSIR produces the highest root mean squared errors, widest 95% BCIs and the lowest coverages of all types of BCIs. Note that only BayesSIR estimates the recovery rate and does it well, as shown in the last row of Table 2. Our simulation results show that a pure birth approximation to the SIR with inhomogeneous mixing leads to bias and poor frequentist calibration of BCIs. Further, using the negative binomial distribution exaggerates these problems further and in addition reduces estimation precision.

### 3.3 London Measles Case Study

We apply our method to the classic measles dataset studied by Finkenstädt and Grenfell (2000). This dataset contains biweekly incidence reports of measles cases between 1944 and 1964. The time series shows the cyclic pattern of measles transmission across years, which was hypothesized to be related to the school calendar. In particular, previous studies have identified lower infection rates during school breaks compared to school terms (Klinkenberg et al., 2018). We are interested in revisiting this question when comparing BayesSIR and BayesTSIR.

Our approach requires computation of the transition probabilities to obtain the likelihood function (5). However, computing these exact SIR transition probabilities using MultiBD for the BayesSIR method

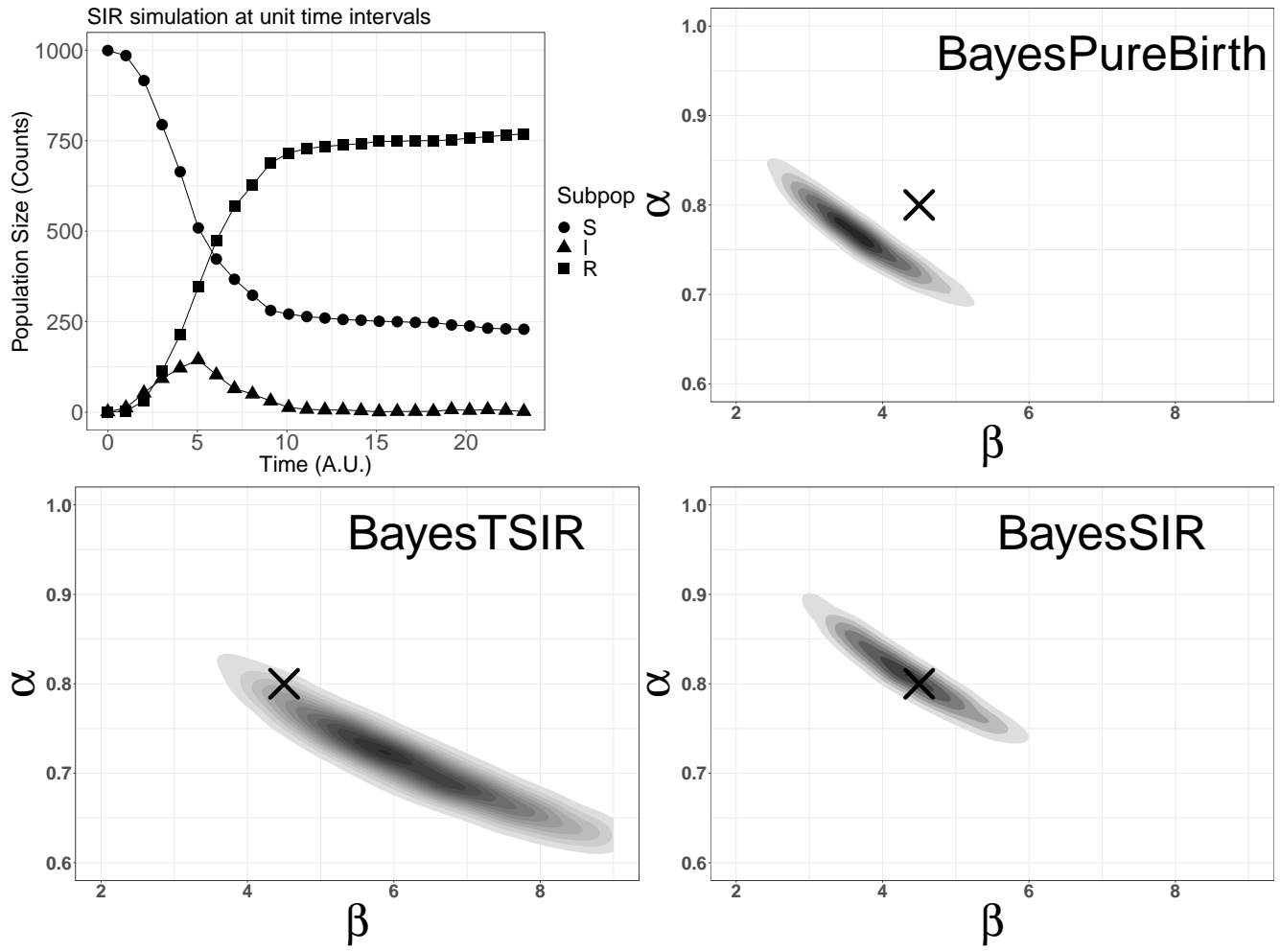


Figure 3: Statistical inference for simulated prevalence data under non-homogeneous mixing. **Top Left:** Example of simulated stochastic SIR trajectories with initial conditions  $S_0 = 999$ ,  $I_0 = 1$  and parameters  $\alpha = 0.8$ ,  $\beta = 0.0045$ ,  $\gamma = 1$ . **Remaining subfigures:** Joint posterior distributions of mixing ( $\alpha$ ) and infection ( $\beta$ ) rates obtained with BayesPureBirth, BayesTSIR and BayesSIR methods. For BayesSIR, the posterior median for  $\gamma$  was estimated to be 1.045 with a 95% Bayesian credible interval (0.9693, 1.128). Note that this parameter was estimated by neither BayesPureBirth nor BayesTSIR. The cross designates the true parameter values used in the simulation.

Table 2: Simulation study results. We generated 629 trajectories of a SIR stochastic process using parameters  $\alpha = 0.8$ ,  $\beta = 0.0045$ , and  $\gamma = 1$ , similarly to the simulation shown in Figure 3. Then, we used BayesTSIR, BayesPureBirth and BayesSIR and likelihood formulations to approximate their corresponding posterior distributions of these parameters using MCMC. For each parameter and method specified, we report the Root Mean Squared Errors (RMSEs) of the posterior median, mean widths of the 95% Bayesian credible intervals (BCIs), and the coverage proportions for BCIs at the 80%, 90% and 95% credible levels.

Parameter	Method	RMSE	Mean width		Coverage	
			95% BCI	80%	90 %	95%
$\alpha$	BayesTSIR	0.13	0.25	0.23	0.35	0.49
	BayesPureBirth	0.07	0.16	0.45	0.57	0.66
	BayesSIR	0.05	0.18	0.76	0.87	0.92
$\beta$	BayesTSIR	3.73	8.69	0.23	0.38	0.49
	BayesPureBirth	0.89	3.02	0.69	0.79	0.84
	BayesSIR	1.06	3.83	0.77	0.87	0.93
$\gamma$	BayesSIR	0.04	0.15	0.78	0.90	0.95

is problematic since high SIR compartment counts (on the order of millions) make repeated evaluation of transition probabilities during MCMC computationally prohibitive. To make this problem tractable, we first take a subset of the data by only considering years 1944–1951. Next, we divide the incidence cases by 100 and round them to the nearest integer as shown in Figure 4. This down-scaling is reasonable since we still preserve the same measles dynamics, including seasonality, but artificially reduce the size of the population under surveillance.

The first step in our analysis is the estimation of the numbers of susceptible and latent infectious individuals. For this purpose, we use the tSIR package (Becker and Grenfell, 2017) to estimate the susceptible population ( $\mathbf{S}$ ), the reporting probability ( $\rho$ ), and the true number of infections ( $\mathbf{I}$ ) from the incidence records shown in Figure 4.

Following previous analyses of this dataset, we assume that the infection rates are not identical throughout the year but the mixing and removal rates remain constant. In particular, we consider two types of seasonality: *schoolterm*, which depends on whether schools are in session or not (corresponding to two infectious rates) and *standard*, which consists of 26 biweeks in a typical year (corresponding to one infectious rate per biweek). For the standard seasonality model, TSIR is able to estimate 26 infectious rates (following the generalized linear model implementation in the R package tSIR). However, due to computational challenges for estimating the transition probabilities using MultiBD, we only computed 13 infectious rates which corresponds to roughly one infectious rate every four weeks. For consistency, we parameterized all methods to include 13 infectious rates.

We use the BayesSIR method to estimate the infection, mixing, and removal rates for the measles dataset. Assuming the schoolterm seasonality model, we estimate two infection rates  $\theta_{schoolterm} = (\alpha, \beta_{schoolbreak}, \beta_{schoolterm}, \gamma)^t$ . Similarly, for the standard seasonality model, we estimate the parameters  $\theta_{standard} = (\alpha, \beta_1, \beta_2, \dots, \beta_{13}, \gamma)^t$ . We use the BayesTSIR with the same settings, except this method does estimate the removal rate  $\gamma$  and sets it to 1.0 instead, because the inter-observation time interval length roughly matches measles mean infectious period of two weeks. We use the Metropolis-Hastings algorithm to approximate the posterior distribution (4) for both models where we use independent  $\text{LogNormal}(0, 100^2)$  priors for all the parameters.

Figure 5 shows the estimated 95% credible intervals for the infection rates of BayesTSIR and BayesSIR under the *schoolterm* model of seasonality. The BayesTSIR exaggerates the decrease in the infection rate during school breaks compared to BayesSIR. Moreover, BayesTSIR results in wider credible intervals for both infection and mixing rates compared to the BayesSIR estimates (Figure 5 and Table 3). We include in Figure S-2 the infection rate 95% confidence intervals produced by the TSIR method as a reference,

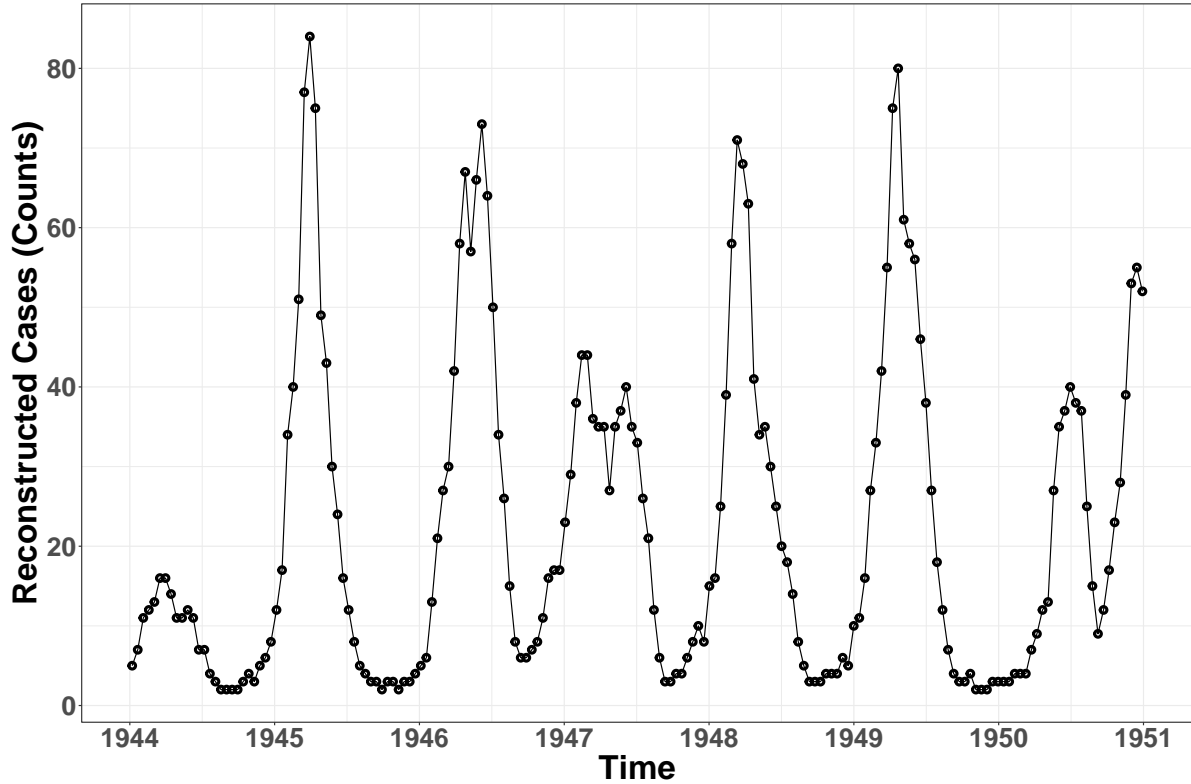


Figure 4: Reconstructed London measles dataset from 1944 to 1951 after applying a rescaling factor of 100 to the original time series.

Table 3: Estimated mixing ( $\alpha$ ) and recovery ( $\gamma$ ) rates for the subsampled London measles dataset. We report the posterior median and the 95% Bayesian credible intervals (BCIs) for the BayesSIR and BayesTSIR methods. We also report TSIR point estimates (\*) of these parameters calculated using the `tsiR` R package (Becker and Grenfell, 2017).

Seasonality	Method	Mixing rate $\alpha$		Recovery rate $\gamma$	
		Median	95% BCI	Median	95% BCI
Schoolterm	BayesSIR	0.965	(0.922, 1.01)	0.99	(0.98, 1.02)
	BayesTSIR	0.945	(0.888, 1.00)	–	–
	TSIR	0.998*	–	–	–
Standard	BayesSIR	0.915	(0.861, 0.973)	0.991	(0.959, 1.026)
	BayesTSIR	0.941	(0.866, 1.014)	–	–
	TSIR	0.974*	–	–	–

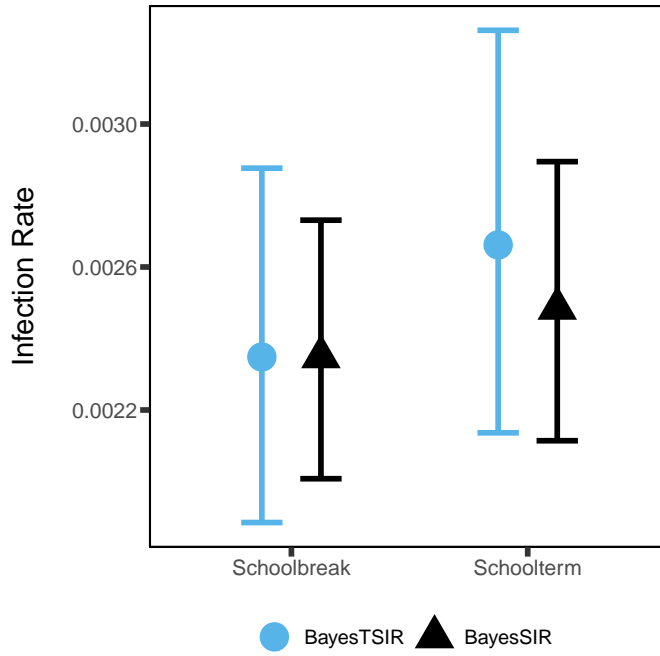


Figure 5: Posterior means (circles and diamonds) and 95% posterior credible intervals (vertical lines with whiskers) for school term and school break infection rates estimated by BayesSIR and BayesTSIR methods from the subsampled London measles data under the *schoolterm* seasonality model.

where we observe a similar pattern. Note that the BayesSIR estimates the removal rate are approximately 1.0 as shown in Table 3.

When we consider the *standard* seasonality model, we observe that BayesTSIR once again exaggerates the decrease in the infection rate during a typical academic summer break (July–September) when compared to the BayesSIR estimates as shown in Figure 6. Figure S-3 shows that the frequentist TSIR model exaggerates the school break effect on measles transmission even more. Table 3 indicates that BayesSIR provides stronger evidence in favor of non-homogeneous mixing under the standard seasonality model than its BayesTSIR counterpart, whose 95% Bayesian credible interval for the mixing rate  $\alpha$  contains 1.0.

## Discussion

In this paper, we study the statistical implications of relaxing the non-homogeneous mixing assumption when estimating infection and mixing parameters from incidence time series data with the help of the TSIR model. The results show that the transition probabilities from the TSIR negative binomial model and those from a stochastic SIR model are close to each other only in the homogeneous mixing regime ( $\alpha = 1$ ). In the presence of non-homogeneous mixing ( $\alpha < 1$ ) using the negative binomial model results in an intentional and undesirable model misspecification. Using simulated data, we demonstrate that this model misspecification results in bias and incorrect quantification of uncertainty in the infection and mixing rates. In contrast, by using either accurate numerical approximations of the correct SIR transition probabilities, or to a lesser extent the non-linear pure birth approximation of the SIR model, we obtain more accurate estimation of the model parameters and better quantification of uncertainty under non-homogeneous mixing. An interesting avenue for future research would be investigating the effect of TSIR negative binomial approximation on forecasting accuracy and calibration under this class of models.

We use TSIR and MultiBD likelihood approximations in a Bayesian framework to estimate the infec-

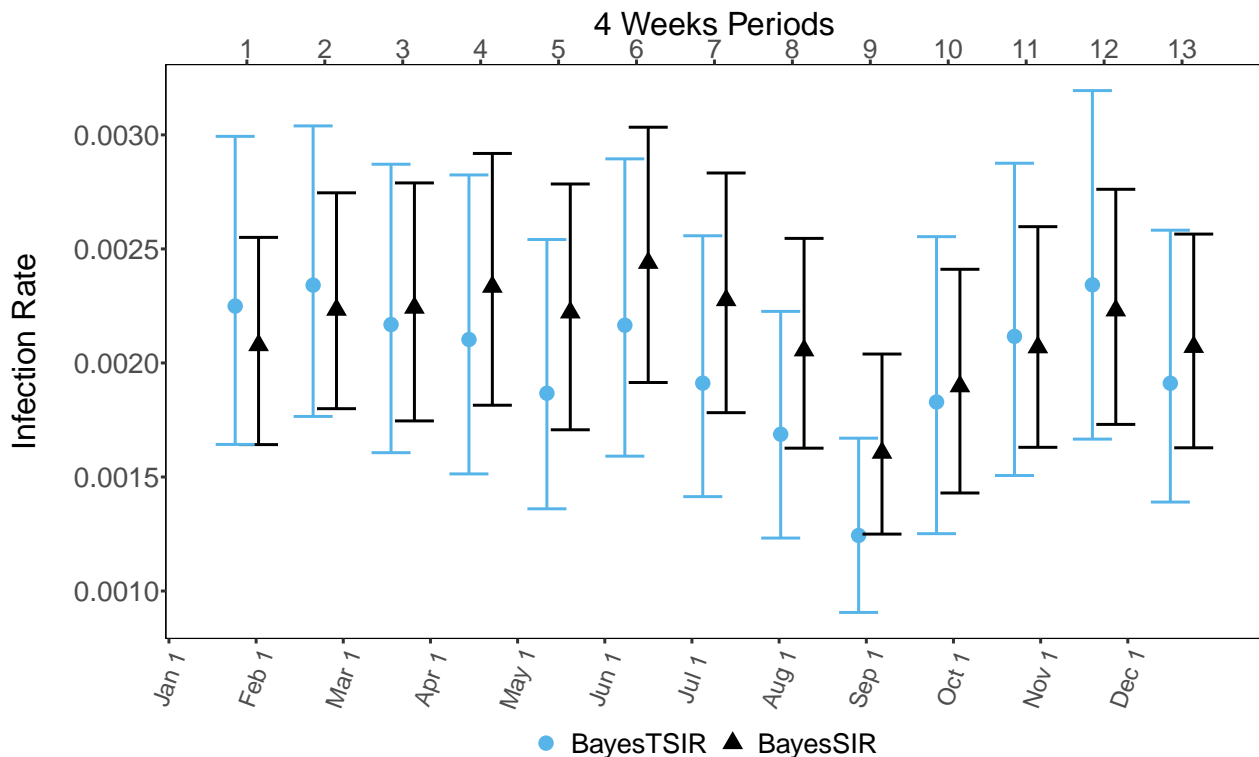


Figure 6: Posterior means (circles and diamonds) and 95% posterior credible intervals (vertical lines with whiskers) for infection rates estimated by BayesSIR and BayesTSIR methods from the subsampled London measles data under the *standard* seasonality model.

tion, mixing and recovery rates from a subset of the historic London measles dataset. Our results show that *BayesTSIR* estimates an exaggerated decrease in the infection rate during academic school break periods compared to *BayesSIR*. However, *BayesSIR* reliance on the `MultiBD` packages makes this method computationally intensive, and currently, it can only be applied to datasets with a moderate number of incidence cases (at most hundreds). In contrast, the negative binomial likelihood from the *BayesTSIR* is computationally efficient due to the simple analytical form of the transition probabilities.

In conclusion, we showed that results of TSIR models with non-homogeneous mixing should be interpreted with caution. It is tempting to assume that these models approximate the canonical stochastic SIR models with non-homogeneous mixing, but it is not the case. A non-linear pure birth process would be a valid approximation, but this approximation does not buy us much in computational efficiency, because its corresponding transition probabilities are not available in closed form and need to be computed numerically. When analyzing data from small populations using models with not too many compartments, accurate numerical methods for computing their corresponding transition probabilities, implemented in the `MultiBD` package, are attractive. When analyzing surveillance data collected from large populations, we recommend resorting to either particle filter algorithms (Andrieu et al., 2010; Ionides et al., 2015) or to principled approximations of stochastic epidemic models (Fearnhead et al., 2014; Fintzi et al., 2021).

## Acknowledgments

We are grateful to Jason Xu and Lam Ho for their help with the `MultiBD` R package. B.S., L.D.J.M.L, and V.N.M. were supported by the NSF grant DMS 1936833.

## References

- Allen, L. J. (2010), *An Introduction to Stochastic Processes with Applications to Biology*, CRC Press.
- Andrieu, C., Doucet, A., and Holenstein, R. (2010), “Particle Markov chain Monte Carlo methods,” *Journal of the Royal Statistical Society: Series B (Statistical Methodology)*, 72, 269–342.
- Baker, R. E., Mahmud, A. S., Wagner, C. E., Yang, W., Pitzer, V. E., Viboud, C., Vecchi, G. A., Metcalf, C. J. E., and Grenfell, B. T. (2019), “Epidemic dynamics of respiratory syncytial virus in current and future climates,” *Nature Communications*, 10, 1–8.
- Becker, A. D. and Grenfell, B. T. (2017), “tsiR: An R package for time-series Susceptible-Infected-Recovered models of epidemics,” *PloS One*, 12, e0185528.
- Bjørnstad, O. N. and Grenfell, B. T. (2008), “Hazards, spatial transmission and timing of outbreaks in epidemic metapopulations,” *Environmental and Ecological Statistics*, 15, 265–277.
- Cauchemez, S., Carrat, F., Viboud, C., Valleron, A., and Boelle, P. (2004), “A Bayesian MCMC approach to study transmission of influenza: application to household longitudinal data,” *Statistics in Medicine*, 23, 3469–3487.
- Dukic, V., Lopes, H. F., and Polson, N. G. (2012), “Tracking epidemics with Google flu trends data and a state-space SEIR model,” *Journal of the American Statistical Association*, 107, 1410–1426.
- Fearnhead, P., Giagos, V., and Sherlock, C. (2014), “Inference for reaction networks using the linear noise approximation,” *Biometrics*, 70, 457–466.
- Feller, W. (1968), *An Introduction to Probability Theory and its Applications, Volume 1*, Wiley series in probability and mathematical statistics, John Wiley & Sons.
- Finkenstädt, B. F. and Grenfell, B. T. (2000), “Time series modelling of childhood diseases: a dynamical systems approach,” *Journal of the Royal Statistical Society: Series C (Applied Statistics)*, 49, 187–205.
- Fintzi, J., Cui, X., Wakefield, J., and Minin, V. N. (2017), “Efficient data augmentation for fitting stochastic epidemic models to prevalence data,” *Journal of Computational and Graphical Statistics*, 26, 918–929.
- Fintzi, J., Wakefield, J., and Minin, V. N. (2021), “A linear noise approximation for stochastic epidemic models fit to partially observed incidence counts,” *Biometrics*, in press.
- Giles, J. R., Cummings, D. A., Grenfell, B. T., Tatem, A. J., Erbach-Schoenberg, E. z., Metcalf, C. J. E., and Wesolowski, A. (2021), “Trip duration drives shift in travel network structure with implications for the predictability of spatial disease spread,” *PLoS Computational Biology*, 17, e1009127.
- Giles, J. R., zu Erbach-Schoenberg, E., Tatem, A. J., Gardner, L., Bjørnstad, O. N., Metcalf, C. J. E., and Wesolowski, A. (2020), “The duration of travel impacts the spatial dynamics of infectious diseases,” *Proceedings of the National Academy of Sciences*, 117, 22572–22579.
- Grenfell, B. T., Bjørnstad, O. N., and Finkenstädt, B. F. (2002), “Dynamics of measles epidemics: scaling noise, determinism, and predictability with the TSIR model,” *Ecological Monographs*, 72, 185–202.
- Held, L. and Paul, M. (2012), “Modeling seasonality in space-time infectious disease surveillance data,” *Biometrical Journal*, 54, 824–843.
- Ho, L. S. T., Crawford, F. W., and Suchard, M. A. (2018a), “Direct likelihood-based inference for discretely observed stochastic compartmental models of infectious disease,” *Ann. Appl. Stat.*, 12, 1993–2021.

- Ho, L. S. T., Xu, J., Crawford, F. W., Minin, V. N., and Suchard, M. A. (2018b), “Birth/birth-death processes and their computable transition probabilities with biological applications,” *Journal of Mathematical Biology*, 76, 911–944.
- Ionides, E. L., Bhadra, A., Atchadé, Y., King, A., et al. (2011), “Iterated filtering,” *The Annals of Statistics*, 39, 1776–1802.
- Ionides, E. L., Nguyen, D., Atchadé, Y., Stoev, S., and King, A. A. (2015), “Inference for dynamic and latent variable models via iterated, perturbed Bayes maps,” *Proceedings of the National Academy of Sciences*, 112, 719–724.
- Jandarov, R., Haran, M., Bjørnstad, O., and Grenfell, B. (2014), “Emulating a gravity model to infer the spatiotemporal dynamics of an infectious disease,” *Journal of the Royal Statistical Society: Series C (Applied Statistics)*, 63, 423–444.
- Jewell, C. P., Kypraios, T., Neal, P., Roberts, G. O., et al. (2009), “Bayesian analysis for emerging infectious diseases,” *Bayesian Analysis*, 4, 465–496.
- Keeling, M. J. and Ross, J. V. (2008), “On methods for studying stochastic disease dynamics,” *Journal of the Royal Society Interface*, 5, 171–181.
- Kermack, W. O. and McKendrick, A. G. (1927), “A contribution to the mathematical theory of epidemics,” *Proceedings of the Royal Society of London A: Mathematical, Physical and Engineering Sciences*, 115, 700–721, ISSN 0950-1207.
- Klinkenberg, D., Hahné, S. J., Woudenberg, T., and Wallinga, J. (2018), “The reduction of measles transmission during school vacations,” *Epidemiology*, 29, 562–570.
- Koepke, A. A., Longini Jr, I. M., Halloran, M. E., Wakefield, J., and Minin, V. N. (2016), “Predictive modeling of cholera outbreaks in Bangladesh,” *The Annals of Applied Statistics*, 10, 575.
- Lekone, P. E. and Finkenstädt, B. F. (2006), “Statistical inference in a stochastic epidemic SEIR model with control intervention: Ebola as a case study,” *Biometrics*, 62, 1170–1177.
- Longini Jr, I. M. and Koopman, J. S. (1982), “Household and community transmission parameters from final distributions of infections in households,” *Biometrics*, 38, 115–126.
- McKinley, T., Cook, A. R., and Deardon, R. (2009), “Inference in epidemic models without likelihoods,” *The International Journal of Biostatistics*, 5, 1–40.
- O’Neill, P. D. (2010), “Introduction and snapshot review: relating infectious disease transmission models to data,” *Statistics in medicine*, 29, 2069–2077.
- Owen, J., Wilkinson, D. J., and Gillespie, C. S. (2015), “Likelihood free inference for Markov processes: a comparison,” *Statistical Applications in Genetics and Molecular Biology*, 14, 189–209.
- Toni, T., Welch, D., Strelkowa, N., Ipsen, A., and Stumpf, M. P. (2009), “Approximate Bayesian computation scheme for parameter inference and model selection in dynamical systems,” *Journal of the Royal Society Interface*, 6, 187–202.
- Wakefield, J., Dong, T. Q., and Minin, V. N. (2019), “Spatio-temporal analysis of surveillance data,” in *Handbook of Infectious Disease Data Analysis*, edited by L. Held, N. Hens, P. D O’Neill, and J. Wallinga, pages 455–476, Florida, USA: CRC Press.
- Xia, Y., Bjørnstad, O. N., and Grenfell, B. T. (2004), “Measles metapopulation dynamics: a gravity model for epidemiological coupling and dynamics,” *The American Naturalist*, 164, 267–281.



## Supplementary Material

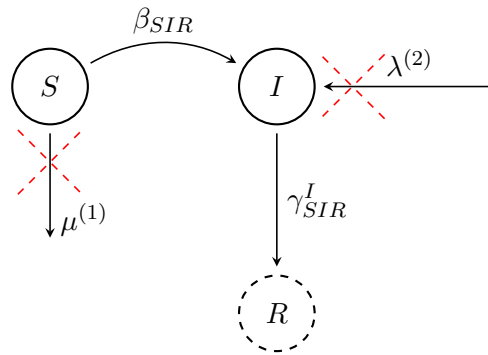


Figure S-1: Graphical representation of a SIR compartmental model as a birth/birth-death process for a time step  $(t, t + \Delta t)$ , where  $\lambda^{(2)}$ 's is the birth rate,  $\mu^{(1)}$  is the death rate,  $\beta_{SIR}$  is the infection rate and  $\gamma_{SIR}^I$  is the recovery rate. In this formulation, a susceptible individual can either stay susceptible or become infected, and an infectious individual can either stay infectious or become recovered. This representation of a SIR model allows us to re-parameterize it in terms of new infections  $nSI$  and new recoveries  $nIR$  and associated transition probabilities using MultiBD.

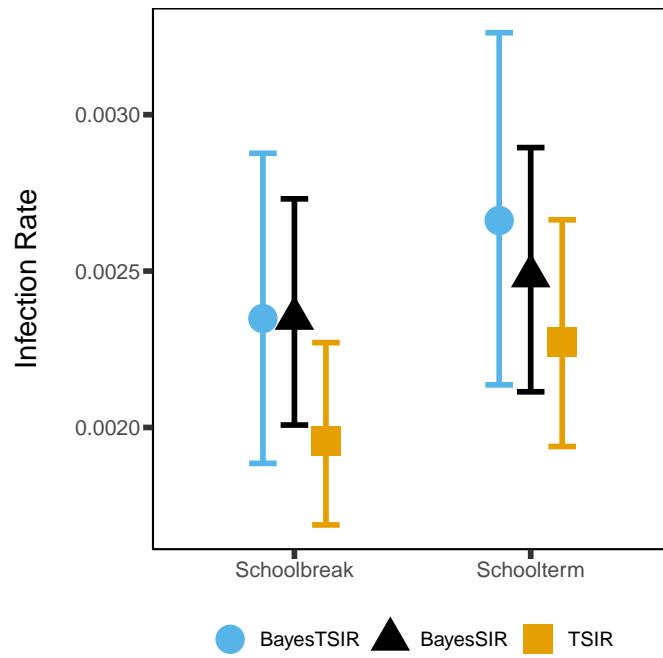


Figure S-2: Estimated infectious rates means (marks) and 95% credible intervals (errorbars) for schoolterm vs. schoolbreak seasonality calculated using the Bayesian TSIR negative binomial model (BayesTSIR) and the Bayesian SIR model with MultiBD (BayesSIR) for the measles dataset from 1944 to 1951. The TSIR 95% confidence intervals from the tSIR package are included for reference.

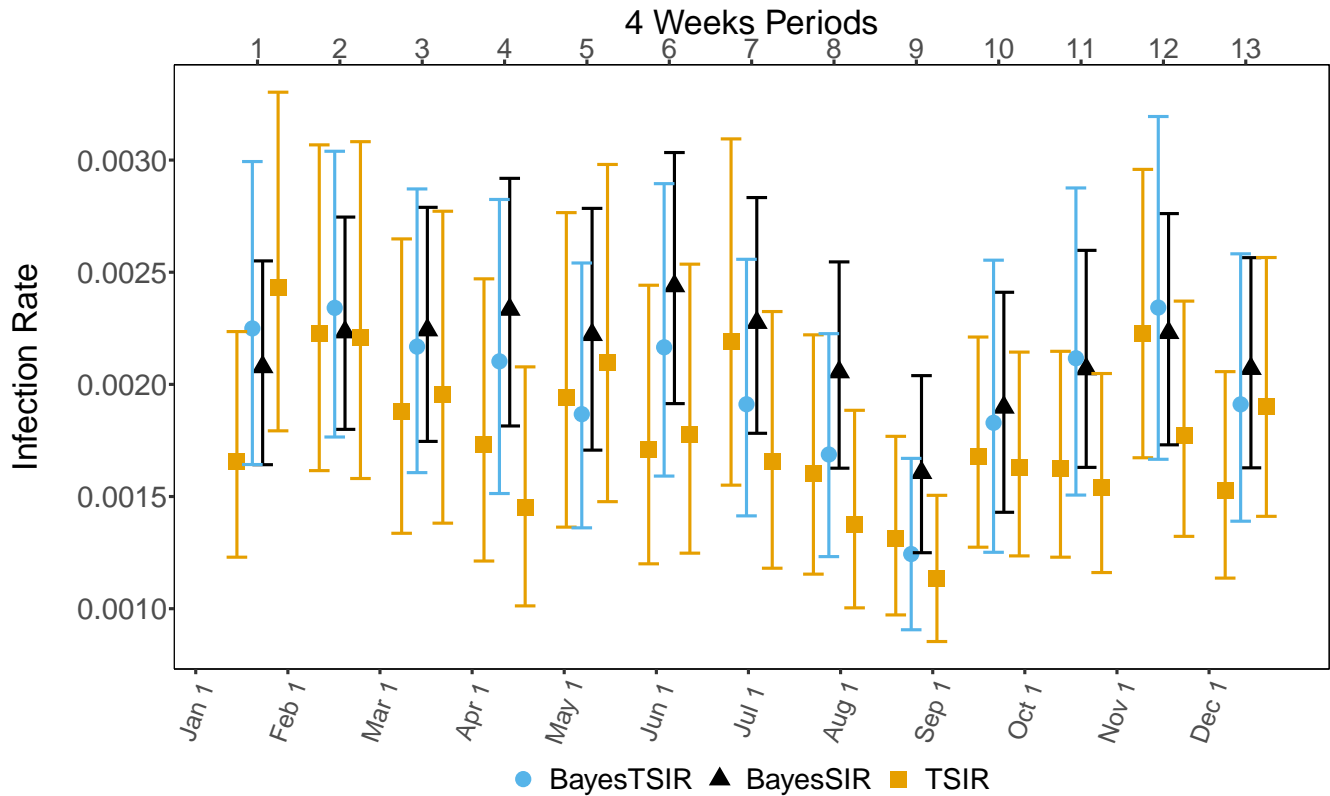


Figure S-3: Estimated infectious rates means (marks) and 95% credible intervals (errorbars) shown every 4 weeks periods calculated using the Bayesian TSIR negative binomial model (BayesTSIR) and the Bayesian SIR model with MultiBD (BayesSIR) for the measles dataset from 1944 to 1951. The TSIR 95% confidence intervals from the tSIR package are included for reference.

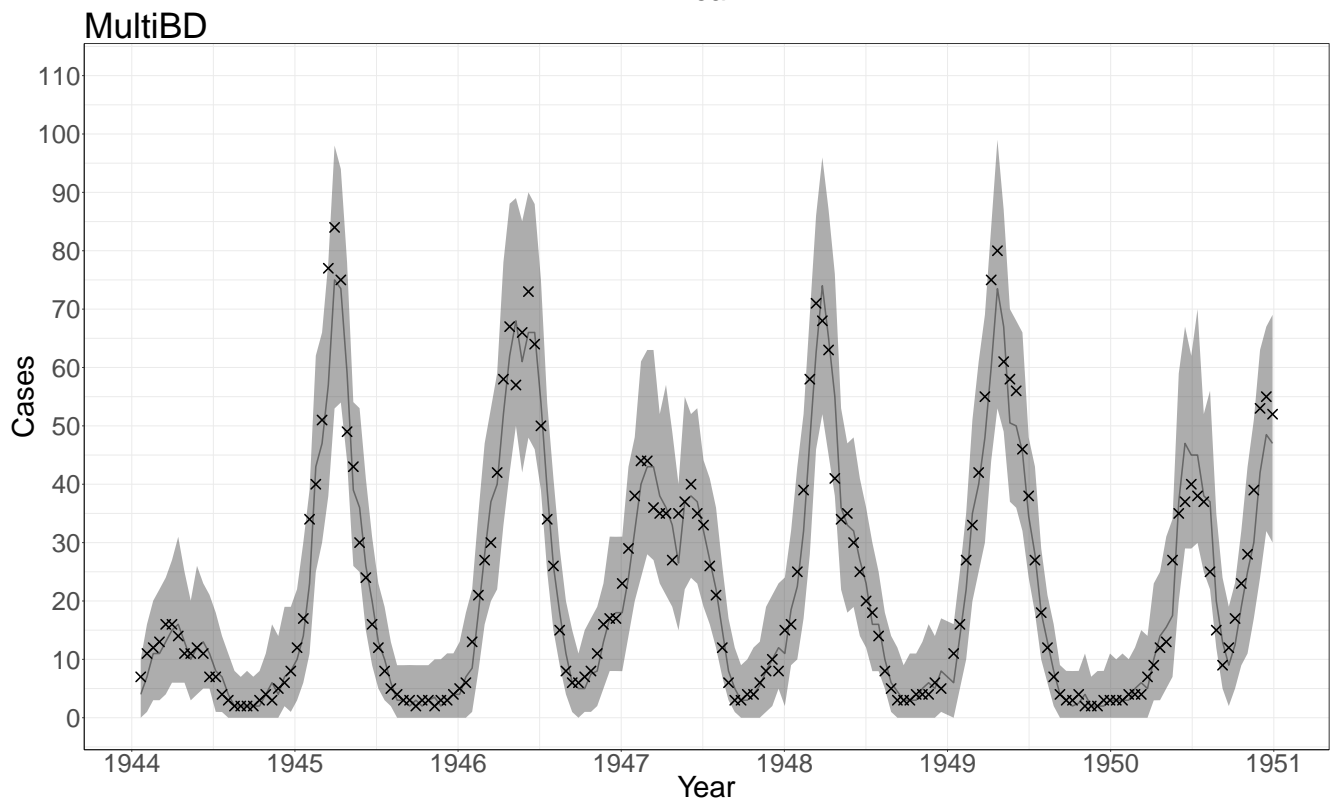
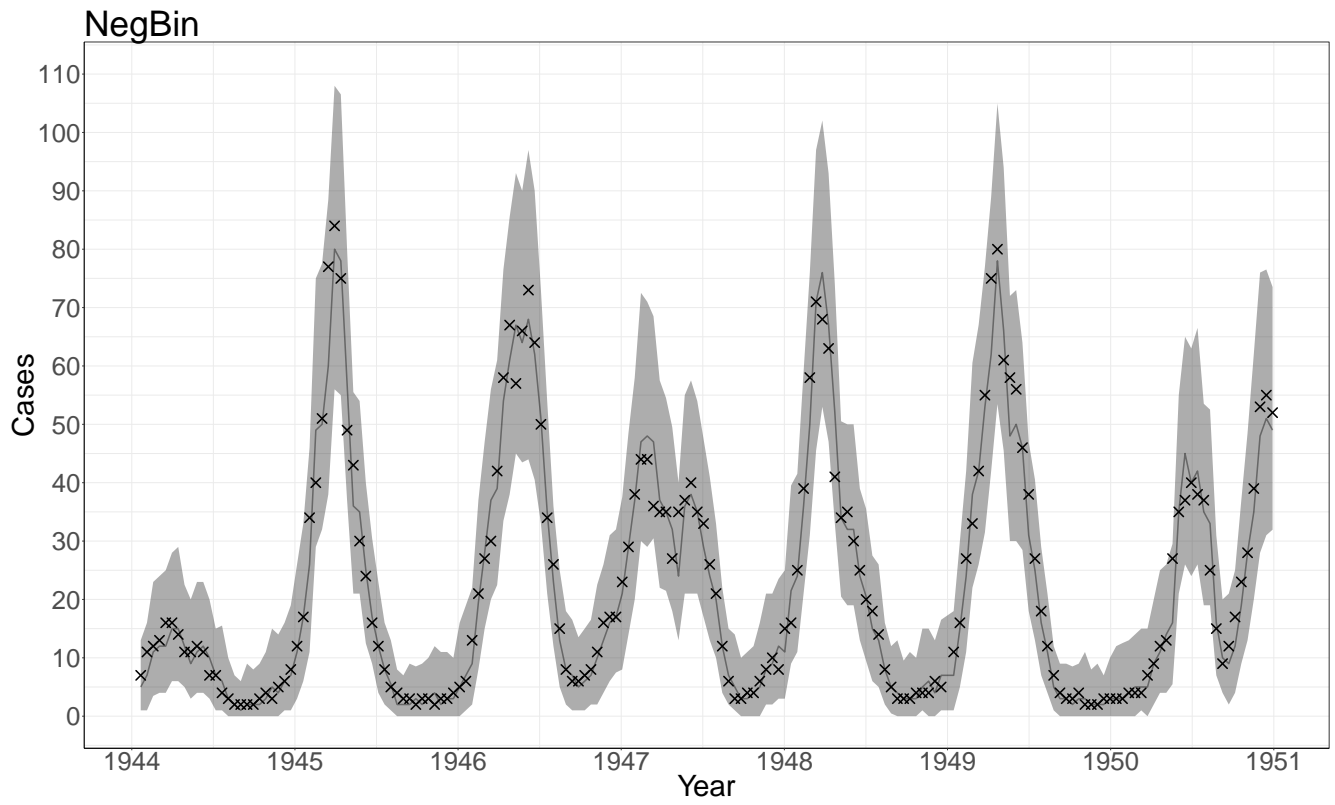


Figure S-4: Posterior predictive checks comparing BayesTSIR vs BayesSIR methods